

This discussion paper is/has been under review for the journal Hydrology and Earth System Sciences (HESS). Please refer to the corresponding final paper in HESS if available.

# Classification of thermal waters based on their inorganic fingerprint and hydrogeothermal modelling

**I. Delgado-Outeiriño<sup>1</sup>, P. Araujo-Nespereira<sup>1</sup>, J. A. Cid-Fernández<sup>1</sup>, J. C. Mejuto<sup>2</sup>, E. Martínez-Carballo<sup>3</sup>, and J. Simal-Gándara<sup>3</sup>**

<sup>1</sup>Geodynamics Group, Marine Geo-science and Territory Rationalization Department, Faculty of Science, University of Vigo, Ourense Campus, 32004 Ourense, Spain

<sup>2</sup>Physical-Chemistry Department, Faculty of Science, University of Vigo, Ourense Campus, 32004 Ourense, Spain

<sup>3</sup>Nutrition and Bromatology Group, Analytical and Food Chemistry Department, Faculty of Food Science and Technology, University of Vigo, Ourense Campus, 32004 Ourense, Spain

Received: 29 March 2011 – Accepted: 15 April 2011 – Published: 5 May 2011

Correspondence to: J. Simal-Gándara (jsimal@uvigo.es)

Published by Copernicus Publications on behalf of the European Geosciences Union.

**HESSD**

8, 4559–4581, 2011

**Classification of  
thermal waters based  
on their inorganic**

I. Delgado-Outeiriño et al.

Title Page

Abstract

Introduction

Conclusions

References

Tables

Figures

◀

▶

◀

▶

Back

Close

Full Screen / Esc

Printer-friendly Version

Interactive Discussion



## Abstract

Hydrothermal features in Galicia have been used since ancient times for therapeutic purposes. A characterization of these thermal waters was carried out in order to understand their behaviour based on inorganic pattern and water-rock interaction mechanisms. In this way 15 thermal water samples were collected in the same hydrographical system. The results of the hydrogeochemistry analysis showed one main water family of bicarbonate type sodium waters, typical in the post-orogenic basins of Galicia. Principal component analysis (PCA) and partial least squared (PLS) clustered the selected thermal waters in two groups, regarding to their chemical composition. This classification agreed with the results obtained by the use of geothermometers and the hydrogeochemical modelling. The first included thermal samples that could be in contact with surface waters and therefore, their residence time in the reservoir and their water-rock interaction would be less important than for the thermal waters of the second group.

## 1 Introduction

Galicia, in northwest Spain and with an area of 29 574 km<sup>2</sup>, is bordered by Portugal to the south, the Spanish regions of Castile and León and Asturias to the east, the Atlantic Ocean to the west, and the Bay of Biscay to the north. Galicia was affected by the Hercynian orogeny and in this region, materials of Proterozoic and the Palaeozoic outcrops are affected by major faults. This Hesperian massif has emerged since the end of the Paleozoic and erosion has exposed important granite batholites.

Galicia has vast mineral-medical resources in its subsoil, as there are more than three hundred sources registered, of which twenty are used by spas (Dirección Xeral de Industria, Enerxía e Minas, 2003). The use of thermal waters in Galicia, for therapeutic means, dates back to Roman times. During the nineteenth century the thermal baths experienced a golden age, with several spas, but at the end of this century a long

**HESSD**

8, 4559–4581, 2011

### Classification of thermal waters based on their inorganic

I. Delgado-Outeiriño et al.

Title Page

Abstract

Introduction

Conclusions

References

Tables

Figures

◀

▶

◀

▶

Back

Close

Full Screen / Esc

Printer-friendly Version

Interactive Discussion



crisis began. present more emphasis is being placed on their recreational and aesthetic aspects than on their curative potential. Recently, Ourense was designated by the Galician Regional Parliament as the Thermal Capital of Galicia due to their therapeutic hot springs, representing the second highest position in thermal water of the Iberian Peninsula.

Most of these sources reach the highest water temperatures in Spain of about 71 °C. The abundance of these springs in Galicia is associated with the lithologic type and the soil fracturation.

The chemistry of thermal waters has attracted the attention of numerous studies to understand the processes that have influence on the recharge of underground water from its origin to estimate its resource importance and potential exploitation. In this way, some studies have been developed with the thermal waters of the area of Ourense city, the Thermal Capital of Galicia due to their therapeutic hot springs (González-Barreiro et al., 2009; Delgado-Outeiriño et al., 2009).

Carballiño is a municipality in the Spanish province of Ourense and has an area of 54 km<sup>2</sup>. It has famous thermal spas together with multiple streams that bathe the countryside.

With the renewed interest in thermomineral waters, the principal aim of this study was to characterize the chemical equilibrium state of waters from Carballiño, as well as the thermodynamic conditions influencing water-rock interaction. As a secondary line of interest, this study aims to determine the temperature of the water within the reservoir.

## 2 Experimental

### 2.1 Geochemical and hydrogeological setting

From the geological point of view, Carballiño is situated on a granite crystalline substrate, which could be divided into two study areas, Northeast and Southwest (Fig. 1).

**HESSD**

8, 4559–4581, 2011

### Classification of thermal waters based on their inorganic

I. Delgado-Outeiriño et al.

Title Page

Abstract

Introduction

Conclusions

References

Tables

Figures

◀

▶

◀

▶

Back

Close

Full Screen / Esc

Printer-friendly Version

Interactive Discussion



The North Eastern part consists of schist with granitic injections and two-mica granite rocks of adamellites, in which several intrusions of gneiss and schist are present. It is in this area where 10 of the 15 selected thermal waters (1-2-3-9-10-11-12-13-14-15) are located. Upwelling of these waters would occur in areas of contact between granite rocks and metamorphic materials (schists). This granitic material is closely associated with metamorphism and migmatization. The granite rocks of adamellites should be formed by anatexis in deeper areas, when the main Hercynian metamorphism reached the maximum temperature.

The most abundant rock material in the Southwest area is one of the most common facies of granite, medium- to coarse-grained porphyritic granodiorite, which is composed of quartz, feldspar, plagioclase, muscovite and biotitic. Only one of the 15 thermal waters is here located, Beran Spa (8), with a temperature of 27 °C (Table 1). The rest of the selected thermal waters are related with the schistose material found in this area (4-5-6-7) with the highest temperatures (>40 °C).

The macro-fracturation of this area is represented by two large families of fractures that intersect with each other. These families correspond to fracture N 20° W and N 130° W. An intense river network uses the lineation of these structures and it is observed along Miño river and also in its tributaries. This is the basis for the thermal circuit and provides the upwelling of springs.

## 2.2 Sampling procedure in thermal water sites

In this study 15 thermal water samples were collected in April 2008 (Table 1).

Water samples were collected by immersing amber glass bottles at the points of emission. All samples were placed in a portable cooler, with ice, immediately after collection to prevent bio alteration; in the laboratory, they were transferred and stored at 4 °C until analysis within the next 24 h.

**HESSD**

8, 4559–4581, 2011

### Classification of thermal waters based on their inorganic

I. Delgado-Outeiriño et al.

Title Page

Abstract

Introduction

Conclusions

References

Tables

Figures

◀

▶

◀

▶

Back

Close

Full Screen / Esc

Printer-friendly Version

Interactive Discussion



## 2.3 Chemical analysis

Temperature, pH and electrical conductivity of waters were measured in the field. Aluminium, boron, caesium, strontium and zinc were determined by Inductively Coupled Plasma Mass Spectrometry (Thermo X series II ICP-MS). Calcium, iron, magnesium and manganese were measured by atomic absorption spectrophotometry (Varian SpectrAA-250 Plus). Lithium, sodium and potassium were analysed by atomic emission spectrophotometry (Varian SpectrAA-250 Plus). Chloride, fluoride, sulphur, nitrite, nitrate, ammonium, phosphate and sulphate anions were determined by capillary electrophoresis (Thermo Capillary Electrophoresis using UV/Vis detector Cristal 100). Bicarbonate was determined by acidimetric titration. Analytical errors are generally <5% for the main components.

## 2.4 Thermal water chemistry

The combined use of  $\text{Cl}/\text{SO}_4$ ,  $\text{Cl}/\text{HCO}_3$  and  $(\text{Cl}+\text{SO}_4)/\text{HCO}_3$  and the Hill-Piper diagram (Piper, 1944) led to an improved classification of the thermal water samples.

The statistical methods used for data analysis of the samples were principal component analysis (PCA) and partial least squares regression (PLS-regression) (López-Chicano et al., 2001; Cruz and França, 2006; Cerón et al., 2009). The PC model was calculated on the auto scaled (namely, columns were mean-centred and scaled to unit variance) data. This was done to focus the analysis on in-between sample variations and unify the importance of each variable independently of the concentration levels. The model was further validated by cross-validation, visual inspection of loadings, and chemical interpretation to ascertain the presence of a meaningful interpretation for the PCA. The method of regression by PLS has been used extensively in chemometrics, where they have found a wide field of application. To attach a weighting to each variable, the data obtained were divided by the standard deviation of each series and later processed by means of PLS2 algorithm of Unscrambler program, utilizing the method of "cross validation". "Leverage correction" validation method may

HESSD

8, 4559–4581, 2011

### Classification of thermal waters based on their inorganic

I. Delgado-Outeiriño et al.

Title Page

Abstract

Introduction

Conclusions

References

Tables

Figures

◀

▶

◀

▶

Back

Close

Full Screen / Esc

Printer-friendly Version

Interactive Discussion



result in over-optimistic validation results. Statistical analysis was carried out using the following statistical programmes: Unscrambler version 9.1 (Camo Process AS, 2004, www.camo.no) and Statgraphics version 5.1 both for Windows.

## 2.5 Geothermometers and hydrogeochemical modelling

5 Silica Geothermometers were used to obtain the most precise data possible about the theoretical reservoir temperature of our system and it was carried out using the thermodynamic database WATEQ4F.dat (Moller and Nordstrom, 2001) included in the PHREEQC package (Parkhurst et al., 1990). The PHREEQC package was also used for the geothermometric modelling.

## 10 3 Results and discussion

### 3.1 Chemical composition of waters and ionic ratios

The measurements taken on thermal waters are reported in Table 1. PH values range from 7.2 to 9.4, indicating alkaline nature thermal waters (Delgado-Outeiriño et al., 2009; López-Chicano et al., 2001). Anions are mostly represented by  $\text{CO}_3\text{H}^-$  (47–366  $\text{mg L}^{-1}$ ), followed by  $\text{CO}_3^{-2}$  (n.d.–57  $\text{mg L}^{-1}$ ),  $\text{Cl}^-$  (9.3–29  $\text{mg L}^{-1}$ ),  $\text{SO}_4^{-2}$  (4.0–38  $\text{mg L}^{-1}$ ),  $\text{F}^-$  (n.d.–16  $\text{mg L}^{-1}$ ) and  $\text{NO}_3^-$  (n.d.–0.91  $\text{mg L}^{-1}$ ). Among the cations,  $\text{Na}^+$  is the main dissolved species (28–97  $\text{mg L}^{-1}$ ), followed mainly by  $\text{Ca}^{+2}$  (2.2–16  $\text{mg L}^{-1}$ ) and  $\text{K}^+$  (0.60–6.6  $\text{mg L}^{-1}$ ). Temperature varies between 13° and 46 °C. The electrical conductivity ranges from 137 to 629  $\mu\text{S cm}^{-1}$ . A global analysis of the inorganic pattern of the selected waters derives in the distinction of only one type of waters as Fig. 2 shows: sodium-bicarbonated waters. Galicia was affected by the hercynian orogeny and these types of waters occur in the internal areas of post-orogenic fracture zones.

Moreover, PCA was carried out to reduce the structure of the data set to two dimensions. The total variance explained by these two components accounts for the 69%

### Classification of thermal waters based on their inorganic

I. Delgado-Outeiriño et al.

Title Page

Abstract

Introduction

Conclusions

References

Tables

Figures

◀

▶

◀

▶

Back

Close

Full Screen / Esc

Printer-friendly Version

Interactive Discussion



(42% PC1 and 27% PC2) of the variability of the data (Fig. 3). The principal plan plot of the selected samples shows two clusters (Fig. 3), which are explained by various factors (chemical and physical water properties). Cluster I is clearly distinct from the other, mainly by their higher  $\text{Ca}^{+2}$ ,  $\text{Mg}^{+2}$ ,  $\text{Fe}^{+2}$ , water hardness and height. The sequence  $\text{Ca}^{+2} > \text{Mg}^{+2} > \text{Na}^{+}$  is similar to the general depth sequence for groundwater composition outlined by Chebotarev (1955). When  $\text{Ca}^{+2} > \text{Mg}^{+2} > \text{Na}^{+}$  it means that young/surface water is present. A young fraction in a confined aquifer suggests possible modern recharge, continuity with surface/shallow waters, or mixing of young and old water. The cluster II contains the water samples that are distinguished due to their temperature,  $\text{S}^{-2}$ ,  $\text{SO}_4^{-2}$ , Si, Li,  $\text{Na}^{+}$  and dry residue contents. In this cluster, the springs belong to Prexigueiro I, II, III, Cortegada and Laias.

Several ratios between different elements were also investigated and the most interesting results were observed between  $\text{Cl}^{-}/\text{SO}_4^{-2}$ ,  $\text{Cl}^{-}/\text{HCO}_3^{-}$  and  $(\text{Cl}^{-} + \text{SO}_4^{-2})/\text{HCO}_3^{-}$  (Table 2). The  $\text{Cl}^{-}/\text{SO}_4^{-2}$  ratio shows the interaction between water and rock (López-Chicano et al., 2001); a higher ratio value would indicate that this water has evolved over much longer time at depth and, therefore, it would interact with the rock. The same conclusion could be drawn with reference to the spatial evolution of the  $\text{Cl}^{-}/\text{HCO}_3^{-}$  and  $(\text{Cl}^{-} + \text{SO}_4^{-2})/\text{HCO}_3^{-}$  ratios (López-Chicano et al., 2001).

The elevated mobility of Li is related to temperature (Chan et al., 1994). It is found in high concentrations in thermal waters, and for this reason it is a good tracer for use in geochemical investigations of hydrothermal systems (Brondi et al., 1973; Brondi et al., 1983). The concentration of Li in water depends on the water-rock contact time (Fidelibus and Tulipano, 1990) and, therefore, Li content could be used as an indicator of the residence time (Edmunds and Smedley, 2000; Sánchez-Martos et al., 2004). Moreover, Leeman and Sisson (1996) found boron in very different geological environments, associated with the presence of volcanic rocks, geothermal processes, and with materials deposited in very saline environments. Because it is highly soluble, it tends to concentrate in environments that have a limited water circulation, like in evaporites or brines of marine or continental origin (Uhlman, 1991). Other authors

## Classification of thermal waters based on their inorganic

I. Delgado-Outeiriño et al.

Title Page

Abstract

Introduction

Conclusions

References

Tables

Figures

◀

▶

◀

▶

Back


Close

Full Screen / Esc

Printer-friendly Version

Interactive Discussion



consider that the elevated boron concentration in some connate waters is directly related to the content of K, *Li*, Mg, Sr and I (Macpherson and Land., 1989). The high values recorded in thermal waters may be due to the  of volcanic rocks and hydrothermal activity (Risacher, 1984; Risacher and Firtz., 1991). In this respect the influence of temperature on its liberation has been noted (Arnorsson and Andresdottir., 1995). In order to find relationships between a set of the main compositional variables (variables *X*) and *Li* or *B* (*Y* variable) for data obtaining from the selected water samples, PLS-R was chosen. The selected algorithm was able to correlate a block of *X* variables with *Li* variable, giving a regression coefficient of 0.9988 for a model with two principal components and 0.8996 with *B* variable. Figure 4 shows a partial squares regression plots. The results obtained show clear separation, based on the first two principal components, between clusters I and II. In cluster I the samples 1, 2, 3, 8, 9, 10, 11, 13 and 14 with lower *Li* and *B* content were grouping. In cluster II the samples 4, 5, 6, 7 and 15 with higher *Li* and *B* content were found. The same clusters were found by PCA with the same distribution and therefore, the same results were found in both analysis. It could be proved that samples of cluster I were the youngest ones or they could be mixing continuity. Nevertheless in cluster II were the samples with longest water-rock contact time.

#### 4 Geothermometer results

One of the most important applications of geochemistry for geothermal resources is using chemical geothermometers to give valuable information about what is happening in the reservoir. The accuracy of a geothermometer application is based on two assumptions. The basic assumption is that a temperature-dependent equilibrium is attained between fluid and minerals in the reservoir. It is further assumed that the composition of a fluid is not affected by chemical reactions in the upflow of geothermal system zones where cooling occurs (Wei, 2006). Various geothermometers have been developed to predict reservoir temperatures in geothermal system (Tole et al., 1993).

### Classification of thermal waters based on their inorganic

I. Delgado-Outeiriño et al.

Title Page

Abstract

Introduction

Conclusions

References

Tables

Figures

◀

▶

◀

▶

Back

Close

Full Screen / Esc

Printer-friendly Version

Interactive Discussion





Geothermometers that have provided better results for these alkaline systems were those based on dissolved silica ( $\text{SiO}_2$ -chalcedony or  $\text{SiO}_2$ -quartz) and Na-K. These two techniques reflect the state of thermal equilibrium solution of these systems with respect to quartz-chalcedony-albite, and potassium feldspar, respectively. In the present work, silica geothermometer was chosen due to the geochemical setting of Galicia.

Table 3 shows the equilibrium temperatures for quartz, chalcedony, kaolinite and k-mica. The chalcedony and/or quartz equilibrium temperatures are also presented for comparison. As can be shown, the calculated temperatures for the quartz chalcedony geothermometers are in the range from 70 to 100 °C and from 30 to 64 °C, respectively. It could be deduced from these results that quartz is the mineral phase, which rules the equilibrium state of the silica, as it was previously reported by Michard (1990), when he studied the behaviour of several elements in deep hot waters from granitic areas of Europe.

Two groups could be distinguished through the results obtained for both geothermometers. The first group would be integrated by the thermal waters, which reached the equilibrium at lowest temperatures (between 70–87 °C for quartz geothermometer and between 33–56 °C for chalcedony geothermometer) and can be shown in table 3 included the samples 1, 2, 3, 8, 9, 10, 11, 13 and 14. The second group formed by the thermal waters 4, 5, 6, 7, and 15, that reached the equilibrium at highest temperatures (between 92–102 for quartz geothermometer and between 62–72 °C for chalcedony geothermometer).

All of these results agree with the previous obtained by PCA and PLSR, where also two groups were found. In group I the selected water samples could be in contact with surface waters and therefore, the time in the reservoir and the water-rock interaction would be less important than for the thermal waters of group II.

#### 4.1 Hydrogeochemical modelling

Geothermometers are based on the assumption that specific temperature-dependent mineral-solution equilibria are attained in the geothermal reservoir. Nevertheless it is

**HESSD**

8, 4559–4581, 2011

### Classification of thermal waters based on their inorganic

I. Delgado-Outeiriño et al.

Title Page

Abstract

Introduction

Conclusions

References

Tables

Figures

◀

▶

◀

▶

Back

Close

Full Screen / Esc

Printer-friendly Version

Interactive Discussion



also advisable to study the fluid saturation equilibrium with the hydrothermal minerals in the reservoir (Reed and Sycher, 1984). In order to know the state of this equilibrium, saturation index (SI) was used and is the logarithm of the ratio (at each temperature) between the solubility product of a certain mineral by hydrolytical reaction ( $Q$ ) and its equilibrium constant ( $K$ ). In this way, the inter-relationship between the lithologies encountered around the waters and their chemical composition could also be explained. All minerals in equilibrium at the same temperature converge to  $SI = 0$ ;  $SI < 0$  for an undersaturated solution, and  $SI > 0$  for a supersaturated solution. In the present work, chalcedony, quartz, calcite, kaolinite and k-mica were selected to calculate the equilibrium state for the selected thermal waters. Table 4 presents the SI for the selected minerals, calculated at the pH and temperature measured in the field. The studied waters are saturated with respect to quartz, k-mica, chalcedony and kaolinite, with the exception of Cortegada Baños and Partovia I. Other authors (López-Chicano et al., 2001) have been also observed super-saturation with respect to quartz in geothermal fluids in Southern Spain. The lower saturation indices observed for chalcedony could be explained to its lower water solubility. The thermal waters 1, 2, 3, 5, 6, 8, 12, 13, 14 and 15 are under-saturated with respect to calcite whereas the samples 4, 7, 9, 10 and 11 and are super-saturated with respect to the same mineral, which is probably due to the cationic change of these thermal waters (D'Amore et al., 1987). Instead, the highest saturation index for kaolinite and K-mica could only be the result of a preferential circulation through feldspar and mica.

In Fig. 5 shows the variation of saturation indices SI with temperature for quartz and chalcedony and kaolinite phases, considering a temperature interval between 20 °C and 120 °C. The intersection of SI curves at zero saturation indexes gives the equilibrium temperature (D'Amore et al., 1987; Tole et al., 1993; López-Chicano et al., 2001). In this way, two groups could be also distinguished through the results obtained depending on the reservoir temperatures for the selected thermal waters. A group formed by the thermal waters, which reach the state of equilibrium at the highest temperatures, between 85 and 110 °C (Fig. 5a) for quartz phases, and between 45 and 85 °C (Fig. 5c)

## Classification of thermal waters based on their inorganic

I. Delgado-Outeiriño et al.

Title Page

Abstract

Introduction

Conclusions

References

Tables

Figures

◀

▶

◀

▶

Back

Close

Full Screen / Esc

Printer-friendly Version

Interactive Discussion



for chalcedony and kaolinite phases. These thermal waters were the samples 4, 5, 6, 7, 12 and 15. The rest of the selected thermal waters would reach the state of equilibrium at the lowest temperatures between, 63 °C and 85 °C (Fig. 5b) for quartz phase, and between 35 °C and 65 °C (Fig. 5d) for chalcedony and kaolinite phases. SI obtained for these samples could depend on re-equilibrium processes during the ascent of the fluid towards the surface.

## 5 Conclusions

In this paper the chemistry of major and trace inorganic elements in 15 thermal waters discharging in the council of Carballiño (province of Ourense) were presented and discussed. The results of the hydrogeochemistry analysis showed one main water family of bicarbonated waters type sodium. Graphical representations of Cl/SO<sub>4</sub>, Cl/HCO<sub>3</sub> and (Cl+SO<sub>4</sub>)/HCO<sub>3</sub> ratios showed interactions between water and rock. These results were proved by PCA and PLSR, where the samples were grouped in two clusters related with the water age and depth. Results of the geothermometric modelling as well as of geothermometers also agreed with the results obtained by the previous analyses and analysis and also two groups of waters were detected. A group formed by thermal waters that reach the equilibrium at highest temperatures (between 85 and 110 °C for IS for quartz and between 92 and 102 °C for quartz geothermometer, and between 45 and 85 °C for IS chalcedony, and between 62 and 72 °C for chalcedony geothermometer), which are under-saturated with respect to calcite. The second group of thermal waters would reach the equilibrium at lowest temperatures (between 63 and 85 °C for IS quartz and 70 and 87 °C for quartz geothermometer, and between 35–65 °C for IS chalcedony and, between 33–56 °C for chalcedony geothermometer) and are super-saturated with respect to calcite. Comparable results were obtained for equilibrium temperatures obtained modelling of the equilibrium states and by geothermometers with an error band of ±10 °C, because of the equilibrium status at depth, chemical reactions at different temperatures (precipitation of kaolinite or calcite).

### Classification of thermal waters based on their inorganic

I. Delgado-Outeiriño et al.

Title Page

Abstract

Introduction

Conclusions

References

Tables

Figures

◀

▶

◀

▶

Back

Close

Full Screen / Esc

Printer-friendly Version

Interactive Discussion



*Acknowledgements.* This work was granted by EU FEDER funds.

## References

- Arnorsson, S. and Andresdottir, A.: Process controlling the distribution of boron and chlorine in natural waters in Iceland, *Geochim. Cosmochim. Ac.*, 59, 4125–4146, 1995.
- 5 Ball, J. W. and Nordstrom, D. K.: User's manual for WATEQ4F, with revised thermodynamic data base and test cases for calculating speciation of major, trace, and redox elements in natural waters, US Geological Survey Open File Report 91–183, USA, 2001.
- Brondi, M., Dall'Aglia, M. D., and Vitrano, F.: Lithium as pathfinder element in the large scale hydrochemical exploration for hydrothermal systems, *Geothermics*, 283(4), 142–153, 1973.
- 10 Brondi, M., Fidelibus, M. D., Gagnan, R., and Tulipano, L.: Hydrochemical study and distribution of some trace elements in the most important coastal springs and groundwater of the Apulian Region (Southern Italy), *Geologia Applicata et Idrogeologia*, XVII (II), 65–80, 1983.
- Ceron, J. C., Puig Bosch, A., and Bakalowicz, M.: Application of principal components analysis to the study of  $\text{CO}_2$ -rich thermomineral waters in the aquifers system of Rio Guadalupe (Spain), 2009.
- 15 Chan, L., Gieskes, J. M., You, C., and Edmond, J. M.: Lithium isotope geochemistry of sediments and hydrothermal fluids of the Guaymas Basin, Gulf of California, *Geochim. Cosmochim. Ac.*, 58, 4443–4454, 1994.
- Chebotarev, I. I.: Metamorphism of natural water in the crust of weathering I, II, and III, *Geochim. Cosmochim. Ac.*, 8, 22–212, 1955.
- 20 Cruz, J. V. and França, Z.: Hydrogeochemistry of thermal and mineral waters springs of the azores archipelago (Portugal), *J. Volcanol. Geoth. Res.*, 151, 382–398, 2006.
- D'Amore, F., Fancelli, R., and Caboi, R.: Observation on the application of chemical geothermometers to some hydrothermal systems in Sardinia, *Geothermics*, 16, 271–282, 1987.
- 25 Delgado-Outeiriño, I., Araujo-Nespereira, P., Cid-Fernández, J. A., Mejuto, J. C., Martínez-Carballo, E., and Simal-Gándara, J.: Behaviour of thermal waters through granite rocks based on residence time and inorganic pattern, *J. Hydrol.*, 373, 329–336, 2009.
- Dirección Xeral de Industria, Enerxía e Minas: Cluster das augas minerais e termais de Galicia. Xunta de Galicia, Consellería de Innovación, Industria e Comercio, 2003.

**HESSD**

8, 4559–4581, 2011

## Classification of thermal waters based on their inorganic

I. Delgado-Outeiriño et al.

Title Page

Abstract

Introduction

Conclusions

References

Tables

Figures

◀

▶

◀

▶

Back

Close

Full Screen / Esc

Printer-friendly Version

Interactive Discussion



- Edmunds, W. M. and Smedley, P. L.: Residence time indicators in groundwater: the East Midlands Triassic sandstone aquifer, *Appl Geochem.*, 15, 737–752, 2000.
- Fidelibus, M. D. and Tulipano, L.: Major and minor ions as natural tracers in mixing phenomena in coastal carbonate aquifers of the Apulia, in: *Proc. Of the 11th Salt Water Intrusion Meeting*, edited by: Kozerski, B. and Sadurski, A., Gandsk, 283–293, 1990.
- González-Barreiro, C., Cancho-Grande, B., Araujo-Nespereira, P., Cid-Fernández, J. A., and Simal-Gándara, J.: Occurrence of soluble organic compounds in thermal waters by ion-trap mass detection, *Chemosphere*, 75, 34–47, 2009.
- López-Chicano, M., Cerón, J. C., Vallejos, A., Pulido-Bosch, A.: Geochemistry of thermal springs, Alhama de Granada (southern Spain), *Appl Geochem.*, 16, 1153–1163, 2001.
- Leeman, W. P. and Sisson, V. B.: Geochemistry of Boron and Its Implications for Crustal and Mantle Processes, *Rev. Mineral.*, 33, 645–707, 1996.
- Macpherson, G. L. and Land, L. S.: Boron in saline brines in Gulf of Mexico sedimentary basin, USA, in: *Water Rock Interaction*, edited by: Balkema, A. A., in the *Proc. 6th Internatl. Sympos. on Water-Rock Interaction*, 457–460, 1989.
- Michard, G.: Behaviour of major elements and some trace elements (Li, Rb, Cs, Sr, Fe, Mn, W y F) in deep hot waters from granitic areas, *Chem. Geol.*, 89, 117–134, 1990,
- Parkhurst, D. L., Thorstenson, D. C., and Plummer, L. N.: PHREEQE – a computer program for geochemical calculations, *US Geol. Surv., Water Resour. Invest.*, 80–96, 1980.
- Piper, A. M.: A graphic procedure in the geochemical interpretation of water analysis, *American Geophysical Union Trans*, 25, 914–923, 1944.
- Reed, M. and Spycher, N.: Calculation of pH and mineral equilibria in hydrothermal waters with application to geothermometry and studies of boiling and dilution, *Geochim. Cosmochim. Ac.*, 48, 1479–1492, 1984.
- Risacher, F.: Origine des concentrations extremes en bore et lithium dans Saumeres de L'Altiplano Bolivie, *R AcadSci Paris Sci de la Terre et des Planets* 299, 701–708, 1984.
- Risacher, F. and Fritz, B.: Geochemistry of Bolivian salars, Lipez, southern Altiplano: origin of solutes and brine evolution, *Geochim. Cosmochim. Ac.*, 55, 687–705, 1991.
- Sánchez-Martos, F., Pulido Bosch, A., Vallejos, A., Molina, L., and Gosbert, J.: Rasgos hidrogeoquímicos de las aguas termales en los acuíferos carbonatados del bajo andarax (almería). *Geogaceta*, 35, 171–174, 2004.
- Tole, M. P., Armannsson, H., Pang, Z.-H., and Arnórsson, A.: Fluid/mineral equilibrium calculations for geothermal fluids and chemical geothermometry, *Geothermics*, 22, 17–37, 1993.

## Classification of thermal waters based on their inorganic

I. Delgado-Outeiriño et al.

Title Page

Abstract

Introduction

Conclusions

References

Tables

Figures

◀

▶

◀

▶

Back

Close

Full Screen / Esc

Printer-friendly Version

Interactive Discussion



Uhlman, K.: The geochemistry of boron in a landfill monitoring program, Ground Water Monitoring Review, 11, 139–143, 1991.

Wei, W.: Geothermal study of the Xianyang low-temperature geothermal field, Shaanxi Province, China, Geothermal Training Programme, 22, 501–522, 2006.

Classification of thermal waters based on their inorganic

I. Delgado-Outeiriño et al.

Title Page

Abstract

Introduction

Conclusions

References

Tables

Figures

◀

▶

◀

▶

Back

Close

Full Screen / Esc

Printer-friendly Version

Interactive Discussion



## Classification of thermal waters based on their inorganic

I. Delgado-Outeiriño et al.

**Table 1.** Sampling sites, and in-site and laboratory measurements of the 15 thermal water samples.

Place (sample)	TM (X)	UTM (Y)	Height (m)	pH	T (°C)	C (μS cm <sup>-1</sup> )	Na <sup>+</sup> mg L <sup>-1</sup>	Li <sup>+</sup> mg L <sup>-1</sup>	K <sup>+</sup> mg L <sup>-1</sup>	Ca <sup>2+</sup> mg L <sup>-1</sup>	Mg <sup>2+</sup> mg L <sup>-1</sup>	Sr <sup>2+</sup> mg L <sup>-1</sup>	Fe <sup>2+</sup> mg L <sup>-1</sup>	Zn <sup>2+</sup> mg L <sup>-1</sup>	B mg L <sup>-1</sup>	WH	Cl <sup>-</sup> mg L <sup>-1</sup>	NH <sup>4+</sup> mg L <sup>-1</sup>	F <sup>-</sup> mg L <sup>-1</sup>	CO <sub>3</sub> <sup>2-</sup> mg L <sup>-1</sup>	Si mg L <sup>-1</sup>	S <sup>2-</sup> mg L <sup>-1</sup>	CO <sub>3</sub> H <sup>+</sup> mg L <sup>-1</sup>	Cs <sup>+</sup> mg L <sup>-1</sup>	Al <sup>3+</sup> mg L <sup>-1</sup>	SO <sub>4</sub> <sup>2-</sup> mg L <sup>-1</sup>	NO <sub>3</sub> <sup>-</sup> mg L <sup>-1</sup>	DR
A Barlos (1)	580734	4695805	352	8.7	21	163	40	0.15	0.94	6.4	0.21	0.10	0.020	0.070	0.26	26	9.5	0.78	5.8	10	26	0.23	60	11	49	6.0	0.13	162
Pontemiza (2)	572372	4697055	345	8.0	17	185	43	0.15	1.2	5.0	0.58	0.09	0.030	0.42	0.38	20	11	1.4	8.3	14	n.d.	n.d.	60	19	35	7.0	0.91	100
Brues (3)	569378	4695511	342	8.3	27	196	43	0.26	1.4	9.2	0.52	0.14	0.020	0.090	0.23	31	14	1.6	7.0	14	33	1.3	57	28	18	16	0.43	176
Presiguero I (4)	568602	4678390	122	8.7	44	363	56	0.57	3.0	4.0	0.25	n.d.	n.d.	0.18	0.63	14	23	2.9	n.d.	33	54	0.71	73	49	60	16	0.37	288
Presiguero II (5)	568794	4678375	122	8.4	29	387	65	0.66	3.5	3.4	0.17	0.060	0.020	0.21	0.91	11	25	2.8	15	31	44	n.d.	112	83	44	38	0.61	352
Presiguero III (6)	568800	4678388	122	8.3	30	369	72	0.77	3.6	3.4	0.06	n.d.	n.d.	0.22	0.70	12	25	4.1	16	30	50	0.40	100	50	52	24	0.18	300
Cortegada Barlos (7)	568265	4672622	92	9.3	40	456	73	1.1	3.5	3.2	0.050	n.d.	0.040	0.25	1.5	14	29	5.7	15	57	42	0.25	116	64	74	16	n.d.	376
Benan Balneario (8)	570392	4688652	161	7.7	27	279	58	n.d.	1.0	5.0	n.d.	n.d.	0.50	n.d.	n.d.	13	16	0.16	n.d.	n.d.	n.d.	n.d.	89	n.d.	n.d.	19	n.d.	240
Partovia I (9)	576648	4695756	335	9.4	37	175	46	0.17	1.0	3.2	n.d.	0.10	n.d.	0.19	0.33	13	11	1.4	5.9	36	31	0.080	47	13	98	10	n.d.	169
Partovia II (10)	576648	4695754	335	9.3	31	179	45	0.17	1.0	3.4	n.d.	0.10	n.d.	0.080	0.24	14	11	1.5	5.5	21	32	0.13	56	16	49	10	n.d.	173
Partovia III (11)	576650	4695738	335	9.2	22	195	45	0.18	1.1	3.2	0.03	0.10	n.d.	0.11	0.36	16	12	1.5	5.3	23	25	0.10	57	8.6	39	11	0.050	170
Gran Balneario (12)	575615	4698320	412	9.2	26	264	28	0.47	0.60	16	n.d.	0.070	0.010	0.090	0.71	58	13	n.d.	5.7	20	26	0.25	95	23	34	10	n.d.	219
Arco Carbaliño (13)	576354	4699769	545	9.0	17	254	54	0.48	2.3	2.2	0.040	0.060	0.070	0.23	16	15	3.5	9.9	32	36	0.040	66	28	46	11	n.d.	238	
O Xarín (14)	576707	4698131	380	7.2	13	137	51	n.d.	1.2	14	11	n.d.	0.020	0.010	0.11	24	9.3	n.d.	4.2	11	21	2.1	51	n.d.	n.d.	9.2	0.21	24
Laas Balneario (15)	579921	4686739	95	7.9	46	629	97	0.96	6.6	6.2	0.38	0.090	n.d.	0.32	0.75	20	24	1.2	n.d.	51	0.16	366	49	70	4.0	0.070	543	

UTM: Universal Transverse Mercator (UTM) coordinates; WH: Water hardness; DR: Dry residue

## Classification of thermal waters based on their inorganic

I. Delgado-Outeiriño et al.

Title Page

Abstract

Introduction

Conclusions

References

Tables

Figures

◀

▶

◀

▶

Back

Close


Full Screen / Esc

Printer-friendly Version

Interactive Discussion



**Table 2.** Some ionic ratios (in  $\text{meq L}^{-1}$ ) of interest in the selected thermal waters.

	$\text{Cl}^-/\text{SO}_4^{2-}$	$\text{Cl}^-/\text{HCO}_3^-$	$(\text{Cl}^- + \text{SO}_4^{2-})/\text{HCO}_3^-$
A Rañoa 	3.2	0.27	0.36
Ponterrizza	4.3	0.32	0.39
Brues	2.3	0.42	0.59
Prexigueiro I	3.9	0.54	0.68
Prexigueiro II	1.8	0.38	0.60
Prexigueiro III	2.3	0.40	0.61
Cortegada Baños	4.8	0.42	0.51
Beran Balneario	2.3	0.31	0.44
Partovia I	2.8	0.38	0.52
Partovia II	2.9	0.33	0.44
Partovia III	2.8	0.35	0.47
Gran Balneario	2.7	0.36	0.49
Arcos Carballiño	3.6	0.38	0.49
O Xardín	2.7	0.31	0.43
Laias Balneario	3.2	0.32	0.45



## Classification of thermal waters based on their inorganic

I. Delgado-Outeiriño et al.

Title Page

Abstract

Introduction

Conclusions

References

Tables

Figures

◀

▶

◀

▶

Back

Close

Full Screen / Esc

Printer-friendly Version

Interactive Discussion




**Table 3.** Quartz, chalcedony, kaolinite and k-mica equilibrium temperatures (°C) using the thermodynamic database WATEQ4F.dat (Ball and Nordstrom, 2001). Equilibrium temperatures for the geothermometers of SiO<sub>2</sub>-quartz and chalcedony are also shown.

Places (sample)	Chalcedony	Quartz	Kaolinite	K-mica	T-quartz	T-chalcedony	Group
A Rañoa (1)	41	73	41		73	41	I
Ponteriza (2)	58	73	60	97	80	49	I
Brues (3)	52	82			83	52	I
Prexigueiro I (4)	65	101	56	82	95	65	II
Prexigueiro II (5)	67	97	58	85	92	62	II
Prexigueiro III (6)	70	103	55	94	95	62	II
Cortegada (7)	70	82	70	72	92	64	II
Beran (8)	40	70	63	81	72	40	I
Partovia I (9)	42	63	35	65	70	48	I
Partovia II (10)	45	75	40	70	72	50	I
Partovia III (11)	35	64	35	64	75	40	I
Gran Bañeal (12)	73	101	45	78	98	71	II
Arcos (13)	54	85	45	75	87	56	I
O Xardín (14)	40	65	65	73	65	33	I
Laias (15)	75	100	85	110	102	72	II

# Classification of thermal waters based on their inorganic

I. Delgado-Outeiriño et al.

**Table 4.** Values of  saturation index for various mineral species using the PHREEQE (Parkust et al., 1990) code.

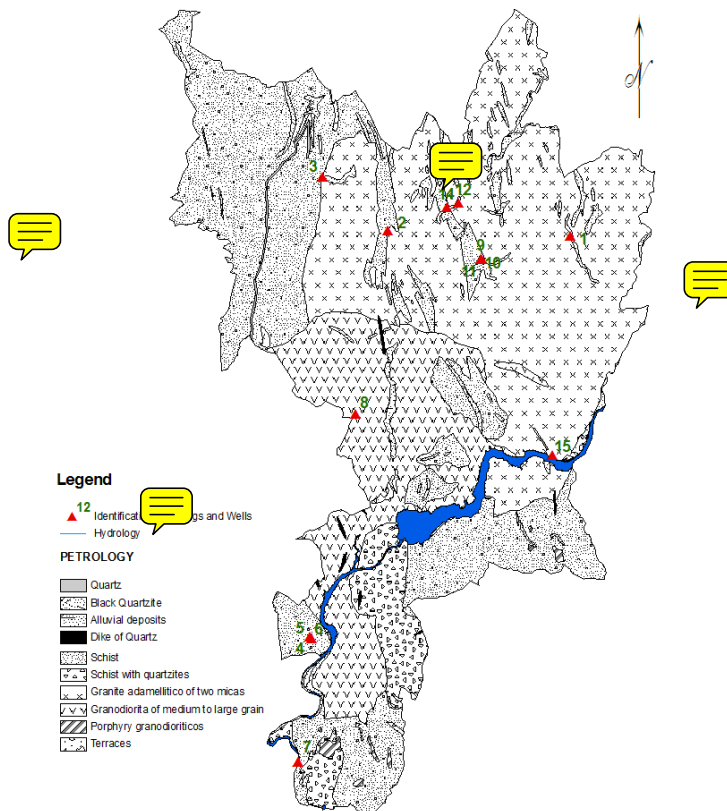


	A Rañoa 1	Ponterriz 2	Brues 3	Prexigueiro I 4	Prexigueiro II 5	Prexigueiro III 6	Cortegada Baños 7	Beran 8	Partovia I 9	Partovia II 10	Partovia III 11	Gran Bañealro 12	Arcos 13	O Xardín 14	Laias 15
Chalcedony	0.220	0.340	0.260	0.320	0.650	0.240	0.0300	0.0800	−0.100	0.0600	0.110	0.400	0.340	0.240	0.250
Quartz	0.660	0.800	0.680	0.710	0.760	0.620	0.420	0.510	0.290	0.470	0.540	0.820	0.800	0.710	0.620
Calcite	−1.04	−2.57	−1.48	0.220	−0.240	−0.350	0.510	−0.600	0.280	0.230	0.0600	−0.110	−0.130	−1.48	−0.530
Kaolinite	8.94	3.58	8.85	0.640	2.27	0.850	−0.440	2.91	−0.380	0.630	1.01	1.46	2.20	3.42	3.45
k-mica	15.7	6.4	15.2	4.60	6.40	4.56	3.31	6.43	2.92	4.22	4.63	5.51	6.65	6.10	7.36

[Title Page](#)
[Abstract](#)
[Introduction](#)
[Conclusions](#)
[References](#)
[Tables](#)
[Figures](#)
[Back](#)
[Close](#)
[Full Screen / Esc](#)
[Printer-friendly Version](#)
[Interactive Discussion](#)


**Classification of  
thermal waters based  
on their inorganic**

I. Delgado-Outeiriño et al.

**Fig. 1.** Hydrogeological map with the sampling sites.

Title Page

Abstract

Introduction

Conclusions

References

Tables

Figures

◀

▶

◀

▶

Back

Close

Full Screen / Esc

Printer-friendly Version

Interactive Discussion



# Classification of thermal waters based on their inorganic

I. Delgado-Outeiriño et al.

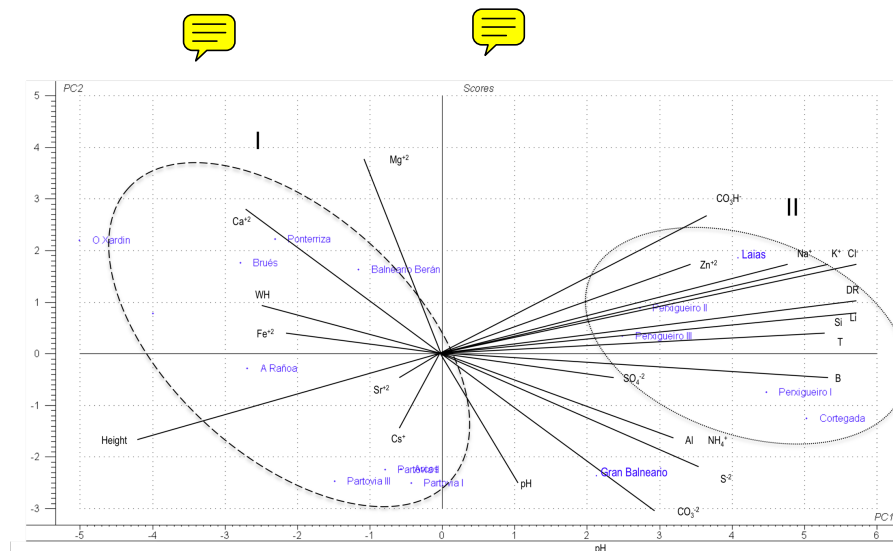


**Fig. 3.** Principal component analysis on the selected thermal waters. Cluster I, samples with the shortest water-rock contact time, lowest equilibrium temperatures and under-saturated with respect to calcite. Cluster II, samples with longest water-rock contact time, highest equilibrium temperature and super-saturated with respect to calcite.

Title Page

Abstract

Introduction

Conclusions

References

Tables

Figures

◀

▶

◀

▶

Back

Close

Full Screen / Esc

Printer-friendly Version

Interactive Discussion



# Classification of thermal waters based on their inorganic

I. Delgado-Outeiriño et al.

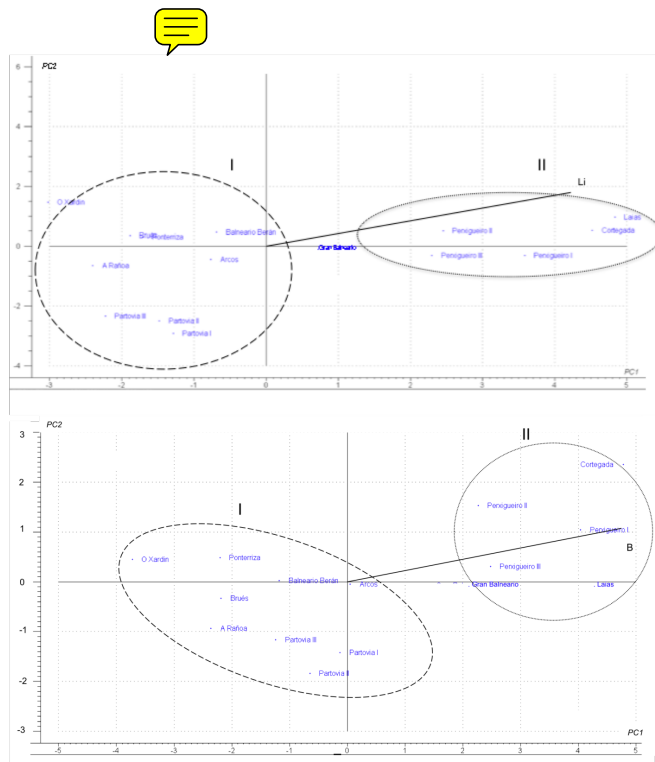


**Fig. 4.** Partial Least-squares regression plots for the selected samples, showing the  $X$  loading weights and the  $Y$  loadings for  $Li$  and  $B$ . Regression coefficient of 0.9988 and 0.8996 for  $Li$  and  $B$ . Two clusters are also distinguished depending on  $Li$  and  $B$  contents.

Title Page

Abstract

Introduction

Conclusions

References

Tables

Figures

◀

▶

◀

▶

Back

Close

Full Screen / Esc

Printer-friendly Version

Interactive Discussion

# Classification of thermal waters based on their inorganic

I. Delgado-Outeiriño et al.

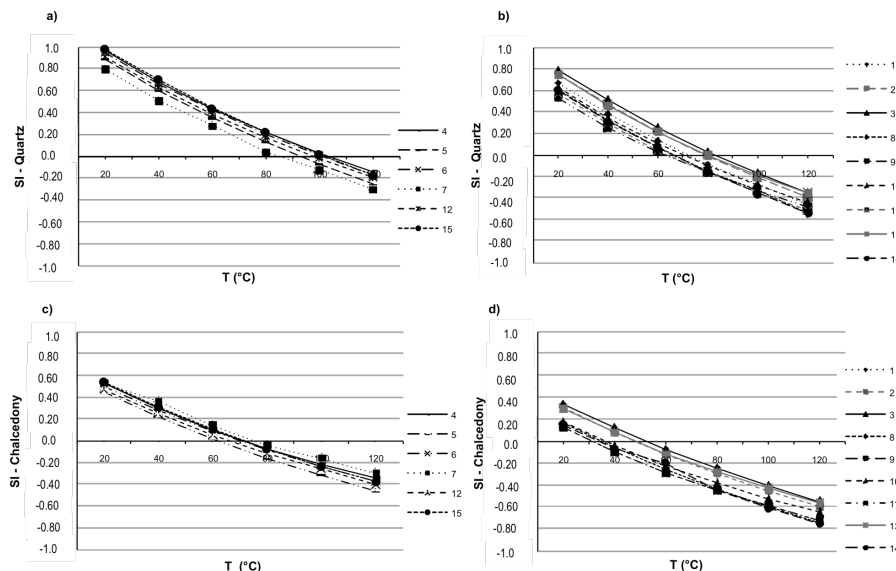


**Fig. 5.** Result of the geothermometric simulations: **(a)** Quartz saturation index for the samples with equilibrium temperature between 85–110 °C, **(b)** Quartz saturation index for the samples with equilibrium temperatures between 63–85 °C, **(c)** Chalcedony saturation index for the samples with equilibrium temperatures between 45–85 °C, **(d)** Chalcedony saturation index for the samples with equilibrium temperatures between 35–65 °C.

Title Page

Abstract

Introduction

Conclusions

References

Tables

Figures

◀

▶

◀

▶

Back

Close

Full Screen / Esc

Printer-friendly Version

Interactive Discussion

